

Fishery and biological characteristics of the pearly hairtail *Trichiurus auriga* Klunzinger, 1884 in the South-eastern Arabian Sea

E. M. Abdussamad, S. Surya*, C. Ramachandran, P. Abdul Azeez, T. B. Rethesh, J. H. Kingsly, K. K. Sajikumar, Jesli Disilva, N. V. Dipti, M. Manoj Kumar, D. Y. Dispin, B. Santhosh and Prathibha Rohit

ICAR-Central Marine Fisheries Research Institute, Ernakulam North P. O, Kochi-682 018, Kerala, India



Abstract

The pearly hairtail *Trichiurus auriga*, a little-known deep-sea ribbonfish, has recently emerged as a commercially relevant resource in southern India due to expanding deep-sea trawling and increasing demand from the fishmeal and fish oil industry. Scientific information on its biology, growth and fishery characteristics remains scarce, limiting management interventions. This study presents the first comprehensive account of fishery trends, age, growth, and reproductive biology of *T. auriga* using specimens (n=895) collected from the Neendakara (Kerala), Colachel and Jeppiar (Tamil Nadu) landing centres between 2022–2024. Length and body weight ranged between 190–420 mm TL (total length) and 20.8–28.4 g respectively. Length-weight relationship (LWR) parameters indicated negative allometric growth ($b = 2.88$), though the deviation from isometry was not statistically significant ($p > 0.05$). Sagittal otolith microstructure analysis revealed ages ranging from 107 to 267 days, with corresponding daily growth rates of 1.34–1.85 mm day $^{-1}$. Female fecundity ranged between 320 and 710 ova, and maturity indicators confirmed sexual maturity at or below 190 mm TL. Large-scale landings and frequent misidentification of *T. auriga* as juveniles of *Trichiurus lepturus*, pose regulatory challenges, particularly in the enforcement of minimum legal size (MLS) regulations. The findings of the study provide baseline biological information and highlight the need for species-specific identification and management strategies to ensure the sustainable exploitation of this emerging deep-sea fishery.



*Correspondence e-mail:
revandasurya@gmail.com

Keywords:

Deep-sea trawling, Fecundity, LWR, Maturity stages, MLS, Ribbonfish, Sagittal otolith

Received : 21.03.2025

Accepted : 26.12.2025

Introduction

Indian coastal fisheries have long supported national food security and livelihood needs; however, in recent decades, have shown high variability and stagnation in production despite continuously increasing demand for marine fish. As coastal resources approached or exceeded sustainable harvest limits, attention progressively shifted towards deeper waters and previously underutilised stocks. Multi-day trawling in India began in the early 1980s, operating in waters up to 200 m depth. From 1999 onward, trawlers were also engaged for deep-sea fishing to depths of around 400 m. As the number of trawlers doubled, their combined engine power became nearly fourfold, from 1980 to 1998 (Najmudeen, 2023). These efforts

consciously expanded to tap non-conventional and underexploited resources and laid the foundation for commercial expansion into deeper waters in later years. This need for diversifying marine resource utilisation led to increased landing and use of lesser-known and underutilised finfish groups. The shift extended specifically toward hitherto under-utilised deep-sea conventional resources such as shrimps, groupers, and snappers (CMFRI, 2022), and a diverse suite of non-conventional resources. These deep-sea resources are physiologically adapted to extreme environments and play ecologically significant roles such as nutrient cycling and carbon sequestration (Ramirez-Llodra *et al.*, 2011). Thus, expanding into deep-sea fishing was viewed as a solution to partly alleviate excessive pressure on heavily exploited nearshore ecosystems. Consequently,

exploiting and utilising previously underutilised groups emerged as a strategic necessity for sustainability.

There remains a substantial scope for the spatial expansion of marine fisheries towards deep-sea and non-conventional resources. Deep-sea fishing fleets regularly encounter several species that contribute to economic returns, including lantern fish (myctophids), unicorn leatherjacket (*Aluterus monoceros*), smooth blaasop (*Lagocephalus inermis*), and red-toothed triggerfish (*Odonus niger*). Ribbonfishes (Family: Trichiuridae) constitute one of the major deep-sea pelagic resources and consistently rank among the top five marine fish groups landed in the country. In 2022, ribbonfish constituted the third most landed marine resource, contributing 226,554 t (6.49%) to national marine fish landings. The fishery is particularly important along the Andhra Pradesh, Karnataka, Goa, Maharashtra, Gujarat, as well as Daman and Diu coasts, where it forms a major component of trawl fisheries. Landings remained substantial in subsequent years, recording 269,616 t (7.64%) in 2023 and 229,359 t (6.62%) in 2024, highlighting the stable economic relevance of this group (CMFRI, 2023, 2024). The ribbonfish fishery in India is dominated mainly by three species; *Trichiurus lepturus*, *T. auriga* and *T. gangeticus*. *T. lepturus* (largehead hairtail) grows to over 100 cm TL and is highly preferred for human consumption, whereas *T. gangeticus* typically support smaller and more regionally confined fisheries. *T. auriga*, in contrast, is substantially smaller (maximum <40–42 cm TL), typically occurring in large shoals along upper slope regions. Due to its smaller size and low fresh-fish market preference, *T. auriga* is mostly diverted to fishmeal and fish oil (FMFO) production rather than table markets (Abdussamad et al., 2023). Nevertheless, in recent years, *T. auriga* has emerged as a major contributor to deep-sea trawl landings in the southern Indian Ocean sector, especially along the coasts of southern Kerala and Tamil Nadu (Abdussamad et al., 2023), indicating its growing economic and fishery relevance.

T. auriga is reported as a marine benthopelagic species with a depth range of about 250–350 m. Its distribution includes the Western Indian Ocean (Red Sea and west coast of India) and parts of the Eastern Indian Ocean (Timor Sea) (Fish base, <https://fishbase.se/summary/Trichiurus-auriga>). Historically, exploratory fishery surveys have documented its abundance. The UNDP/FAO Pelagic Fishery Project-I recorded high availability of pearly hairtails along the shelf edge and upper slope regions of the southern Indian coast extending up to Maharashtra (Silas and Rajagopalan, 1974). FORV Sagar Sampada surveys conducted in 1994 and later in 2014 further confirmed huge landings (8–10 t) from a single trawl haul off Thiruvananthapuram at 200 m depth (Ganga et al., 2015). Surveys by M.F.V. Matsya Varshini of FSI (2004–2005) similarly noted large biomass along deeper waters (100–500 m; 7°–10°N) off the south-west coast of India (Sajeevan and Nair, 2006). More recently, monitoring of deep-sea trawl operations and fisher-derived information indicate extremely high availability of this species along the Thiruvananthapuram–Kanyakumari continental slope, suggesting substantial scope for commercial exploitation (Abdussamad et al., 2023). Ganga et al., (2015) also documented its lucrative occurrence, and Ganga et al. (2024) further confirmed significant landings within the Indian EEZ.

The emergence of *T. auriga* as a non-conventional deep-sea resource in the south-eastern Arabian Sea represents economic potential for a seasonal fishery. Deep-sea trawlers operating at depths of 200–600 m encounter large aggregations forming catch rates averaging 7–10 t per haul,

enabling fishermen to increase profitability through secondary catch during return operations (Abdussamad et al., 2023). Silas and Rajagopalan (1974) and Nakamura and Parin (1993) documented clear morphometric distinctions between *T. auriga* and common ribbonfish *T. lepturus*. However, large landings of small-sized ribbonfishes along the southern Kerala coast, coupled with the enforcement of minimum legal size (MLS) regulations for *T. lepturus*, have led to the frequent misidentification of *T. auriga* as juveniles of the commercially important *T. lepturus*. This misidentification has resulted in regulatory penalties on fishers under the assumption of juvenile exploitation. Reports of this issue from multiple landing centres, highlight the need for detailed biological studies to clearly differentiate the species.

Despite historical records and recent fishery-based indications of abundance, scientific literature on the fishery, biology, age structure, growth and reproductive ecology of pearly hairtails remains extremely limited. This knowledge gap presents a significant challenge to the development of sustainable harvest strategies during the early expansion phase of the fishery. Therefore, it becomes critical to systematically generate biological information on newly emerging fisheries, particularly those in which the majority of landed specimens are small yet reproductively active. Accordingly, the present study aims to provide comprehensive biological information on *T. auriga* from the south-eastern Arabian Sea, thereby supporting evidence-based decision-making to ensure stock sustainability and prevent overexploitation of this rapidly expanding deep-sea fishery. In this study, we additionally provide practical diagnostic characters suitable for rapid field-level identification of *T. auriga*.

Materials and methods

T. auriga (sample size, n=895) were collected from Neendakara Fishing Harbour (Kollam, Kerala) and Colachel and Jeppiar harbours (Kanyakumari, Tamil Nadu), during 2022, 2023 and 2024 and landed by trawlers operated in the Arabian Sea at depths up to 300 m (Fig. 1). The collected samples were transported to the laboratory for ageing and biological studies. In the laboratory, each sample was measured for total length (TL) to the nearest 'cm' and total weight (TW) was recorded to the nearest 'g' using an electronic balance. Identification was verified by comparing morphological traits (fin ray counts, body profile, colour pattern, teeth structure) against authoritative trichiurid identification resources, particularly FAO species catalogue (Collette and Nauen, 1983), snake mackerels and cutlassfishes (Nakamura and Parin, 1993) and general ichthyological taxonomic classification (Nelson, 2006). The length-weight relationship (LWR) was estimated using the equation: $W = aL^b$ (Le Cren, 1951; Ricker, 1973) where W is the total weight (g), L is the total length (cm), and a and b represent the parameters of LWR. The values of 'a' (intercept) and 'b' (slope) were estimated by logarithmic transformation, applying the linearised form: $\log(W) = \log(a) + b \cdot \log(L)$. A linear regression analysis was then performed on log-transformed data to obtain the values of a and b, where b indicates the growth of fish. A value of b = 3 suggests isometric growth, while values significantly different from 3 indicate allometric growth (either positive if b>3 (fish becomes relatively heavier as it grows) or negative if b<3 (fish becomes relatively lighter as it grows)). The coefficient of determination (r^2) was calculated to analyse the goodness of fit. A higher r^2 value suggests a stronger and

more reliable relationship between length and weight, indicating the regression model accurately represents the growth of the fish population studied. A t-test was used to evaluate whether the *b* value significantly differed from the isometric value of 3, with a significance level set at $p < 0.05$. Statistical analyses were performed using 'R' software (Mildenberger *et al.*, 2017).

Longevity analysis using sagittal otoliths

Microstructures on hard parts such as sagittal otoliths were examined using imaging techniques to obtain age and growth data, following standard protocols (Brothers and Mathews, 1987; Green *et al.*, 2009; Abdussamad *et al.*, 2020). After recording the biological characteristics of each specimen, the sagittal otoliths were carefully extracted. The upper portion of the head was removed with a knife to expose the brain cavity. Subsequently, the brain matter was extracted by gently scooping it forward with forceps, exposing the sagittal otoliths, which were then carefully extracted. The otoliths were rinsed in freshwater and stored in labelled plastic tubes filled with alcohol, until analysis. For moulding, each otolith was embedded in epoxy resin, and allowed to harden for 5-6 h prior to sectioning. Each sagittal otolith was embedded ventral side down in the resin block, with the rostrum oriented towards one end. The core region was identified under magnification and marked, after which a 0.3 mm thick section, including the core, was then cut using an

Isomet low-speed saw. The section was sequentially polished with 400- and 600-grit silicon carbide paper, with intermittent rinsing in water until the primordium became clearly visible. After polishing, the section was again rinsed in water, mounted on a glass slide, and observed under a Leica DM6B microscope at $\times 100$ and $\times 1000$ magnifications. Immersion oil was applied to the mounted section to enhance the visibility of growth rings. Ring counts were made from the primordium towards the posterior end of the otolith. For documentation, otolith sections were photographed at $\times 1000$ magnification. Growth rings appeared as alternating opaque and translucent bands, with the opaque rings on the longer arm of the otolith being counted. Daily increments were consistently observed on the sagittal otoliths, with each ring representing one day of growth.

Maturity assessment of *T. auriga*

Fish maturity assessments were conducted during the peak fishing season, which spans 4-5 months annually, as sample availability is limited to this period. During these months, samples were collected for the maturity analysis following Brown-Peterson *et al.* (2011) and Ganga *et al.* (2023). Each dissected gonad was photographed and the microscopic images of oocytes were captured to facilitate visual assessment of maturity as well as to enable comparison with

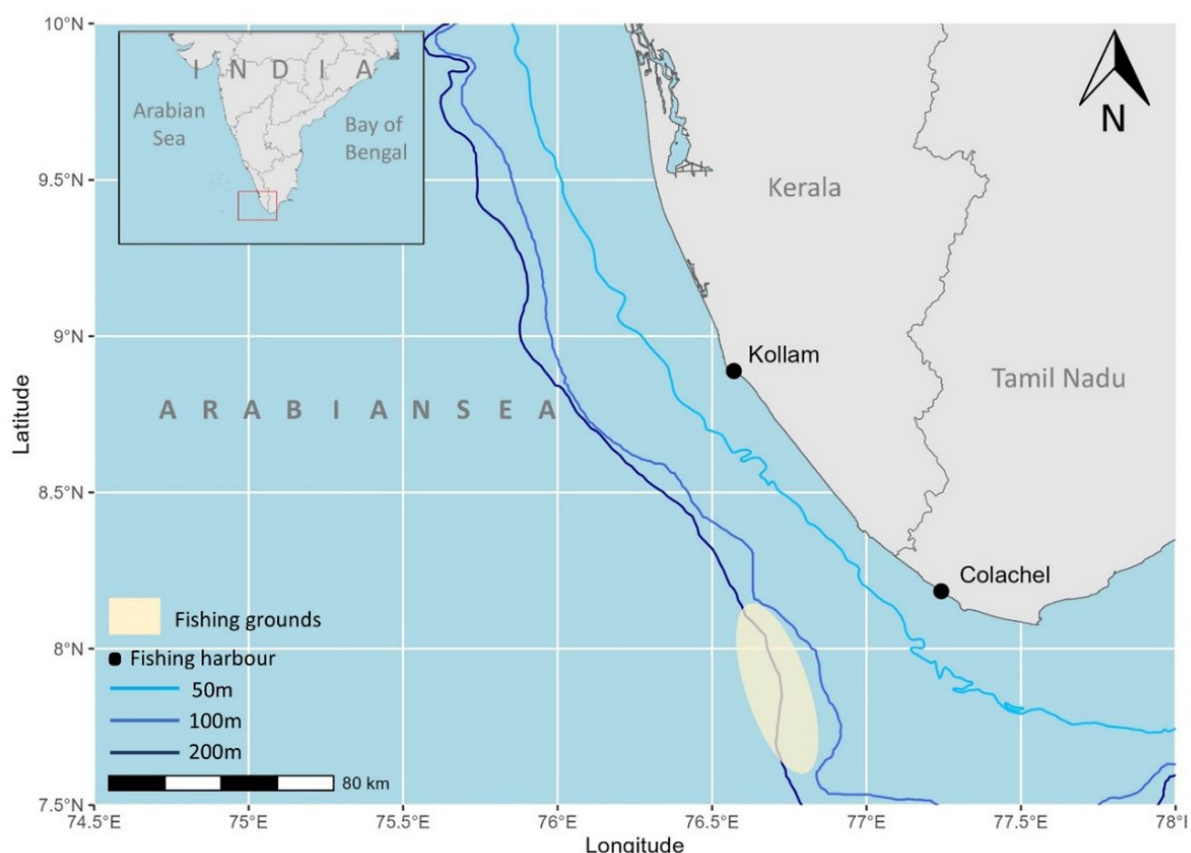


Fig. 1. Sampling sites (Kollam and Colachel) and trawl fishing ground of *T. auriga*

histological observations. Histological analysis served as the primary method to assess maturity, for which fresh gonads were dissected, rinsed in saline to remove adhering fat and blood, cut into approximately 2 mm pieces, and fixed in Bouin's fluid for 2 h. Following fixation, the tissues were washed in running water to remove the yellow colouration and then preserved in 5% formalin for 24 h. The samples were then washed overnight in running water, and gently blotted dry using filter paper. The tissues were then dehydrated by sequential immersion in 70%, 80%, and 90% ethyl alcohol for 1 h each, followed by three changes of 100% ethanol for 1 h each. Subsequently, the tissues were cleared in a 1:1 mixture of absolute alcohol and chloroform, and then transferred to pure chloroform for 30 min. For paraffin embedding, tissues were infiltrated with molten paraffin wax, oriented in molds, allowed to cool, and refrigerated at 4–8°C for 24 h. Sections of 6 µm thickness were cut using a rotary microtome (Leica RM2235, Germany), mounted on glass slides coated with egg albumin, gently warmed to ensure tissue adhesion, and dried for 2–3 h. Dewaxing was performed in xylene (two changes of 4 min each), followed by rehydration through absolute alcohol (4 min), and graded ethanol series of 95%, 90%, 80%, and 70% (2 min each), before rinsing in water for 5 min. Sections were stained with Harris hematoxylin for 5–10 min, rinsed in distilled water, differentiated in acid-alcohol (70% ethanol with HCl) for 1 min, and washed again in distilled water. The slides were then dipped in 1% ammonia water until the sections turned pink, rinsed again in distilled water, and counterstained with eosin (10 dips). Following staining, sections were transferred to 70% ethanol for 10–15 min, followed by two changes each in absolute alcohol and xylene (3 min each) and then mounted using DPX mountant. The prepared slides were examined under a compound microscope (Zeiss PrimoStar with Zen software, Germany) to identify and classify the maturity phases of ovaries and testes.

Results and discussion

Fishery characteristics and exploitation pattern of *T. auriga*

Rising demand from the FMFO sector has led to a sustained requirement for raw materials and the pearly hairtail due to its high abundance and lack of a direct human consumption market, has emerged as a preferred resource. Trawlers operating in the southern regions of Kerala and Tamil Nadu, primarily targeting

shrimps and cephalopods (fishing operation up to 300 m depth), have been catching pearly hairtails during their return journey to optimise deck space utilisation and to enhance economic returns. Targeted fishing for *T. auriga* typically occurs when the species ascends to subsurface waters at depths of 100–150 m during midday (Mr. Jerold, Colachel; pers. comm.), consistent with its diurnal vertical migration. Towing durations range from 30 to 60 min at speeds of 1.5–2 knots, typically involving one or two hauls on the final day of the fishing trip. The average catch of *T. auriga* in such operations generally ranges from 4–5 t per haul. In addition to targeted operations, *T. auriga* incidentally caught during routine trawling operations are also retained, without preservation as it is intended for FMFO processing. This seasonal fishery occurs annually over a four-month period from October to February and there is no consistent consumer market demand for this, except for the FMFO industry. The high availability of *T. auriga* has quickly attracted interest and acceptance from the fishmeal industry, presenting a viable alternative income source for trawlers facing challenges from rising fuel costs and declining profitability. Based on estimates derived from catch rates, vessel capacity, and fishing effort, over 400,000 t of pearly hairtail were reportedly landed between October 2022 and February 2023 (Abdussamad et al., 2023). The fishery continued in the region from November 2023 to March 2024 (Fig. 2).

Taxonomy

Accurately distinguishing *T. auriga* from juveniles of *T. lepturus* remains a critical challenge, especially during periods of substantial landings, when MLS regulations are enforced for the morphologically similar *T. lepturus* and misidentification can lead to inappropriate regulatory actions and unwarranted restrictions on the exploitation of pearly hairtail.

The key distinguishing characteristics between the two species are meristic counts and external morphology. *T. lepturus* typically possesses a greater number of dorsal and anal fin rays (Dorsal: III + 130–137; Anal: 103–115), shows a steely blue metallic sheen with silvery reflections, and exhibits barbed teeth. In contrast, *T. auriga* has comparatively fewer fin rays (Dorsal: III + 106–116; Anal: 83–87), a pearly-white body with a slightly dusky dorsal area, and pointed teeth lacking barbs (Fig. 3; Table 1). In the present study, *T. auriga* samples collected during the fishing seasons of 2022, 2023 and 2024 showed length ranges of 190–420 mm TL. *T. auriga* is distinctly



Fig. 2. Bulk landings of *T. auriga*, at Colachel, Tamil Nadu



smaller, with a maximum reported size of ~420 mm (present study), whereas *T. lepturus* typically ranges from 300 mm to nearly 1 m in commercial landings. In the context of large trawl landings of small-sized ribbonfishes, it is crucial to apply these distinguishing features for accurate species identification. Proper species-level identification is essential for sustainable fisheries management, effective enforcement of MLS-based regulations, and in preventing stock misclassification.

Longevity analysis using sagittal otoliths

Sectioned sagittal otoliths, examined under reflected light, revealed an opaque core encircled by distinct, broad hyaline increments (Fig. 4). Under transmitted light microscopy, alternating dark and

light bands were observed, reflecting diurnal variations in growth patterns resulting from differential mineral deposition. Typically, the dark bands were counted as daily rings for ease of analysis. This observation aligns with findings by Campana and Nelson (1985), who explained how day-night cycles influence fish growth and lead to the formation of these growth rings. In the present study, otoliths consistently displayed regular daily increments with one dark and one light band per day, regardless of the fish size, age, or sex, confirming their reliability for age determination. Al-Anbouri *et al.* (2011) identified such microstructures as daily rings while ageing fish from Oman waters. Similarly, Clain *et al.* (2023) determined the age of *T. lepturus* using sagittal otoliths from the south-eastern Australia.

Based on daily increment counts, the age of the individuals ranged

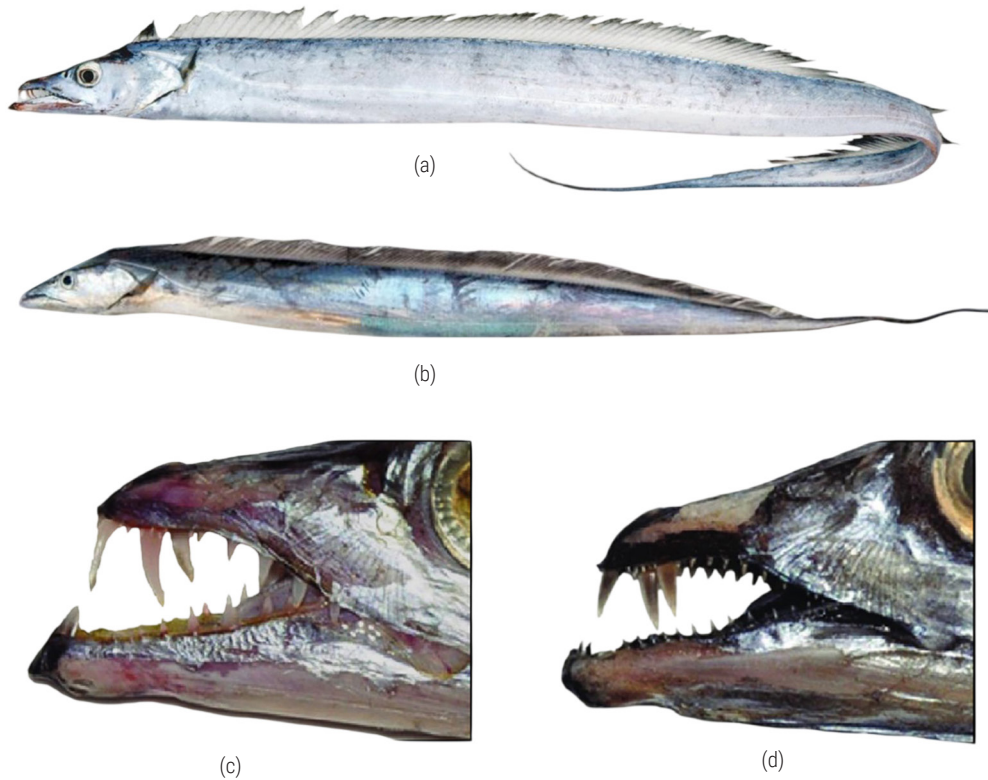


Fig. 3: (a) *T. lepturus*; (b) *T. auriga*; (c) *T. lepturus* teeth with barbs; (d) *T. auriga* pointed teeth without barbs

Table 1. Diagnostic characters separating *T. lepturus* and *T. auriga*

Character / Feature	<i>T. lepturus</i> (Largehead hairtail)	<i>T. auriga</i> (Pearly hairtail)
Dorsal fin rays	III + 130–137	III + 106–116
Anal fin rays	103–115	83–87
Body colouration	Steely blue with silvery reflections	Pearly-white, light dusky dorsal region
Maximum size commonly observed (TL)	80–100 cm (up to ~1 m in landings)	≤42 cm (19–42 cm in present study)
Distribution preference	Coastal to shelf waters, shallower ranges	Upper-slope deepwater habitats (250–350 m)
Dentition	Teeth barbed	Teeth pointed, smooth, without barbs
Commercial utilisation	High edible value; direct consumption	Mostly used for FMFO due to small size
Common confusion	<i>T. auriga</i> (<30 cm), often mistaken as juveniles of <i>T. lepturus</i>	Misidentified as juveniles of <i>T. lepturus</i> in trawl landings

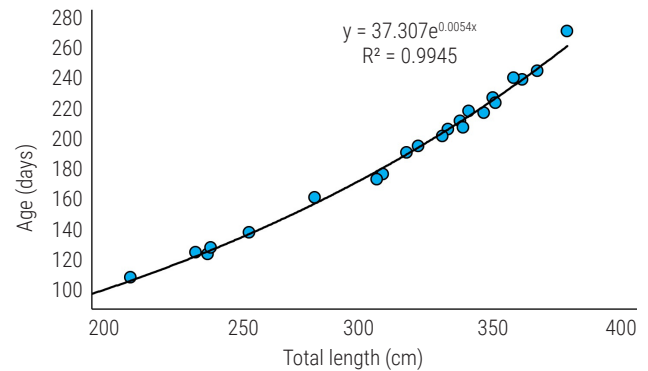
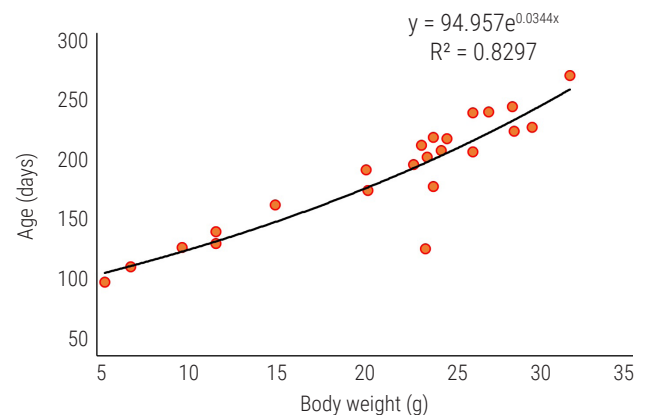
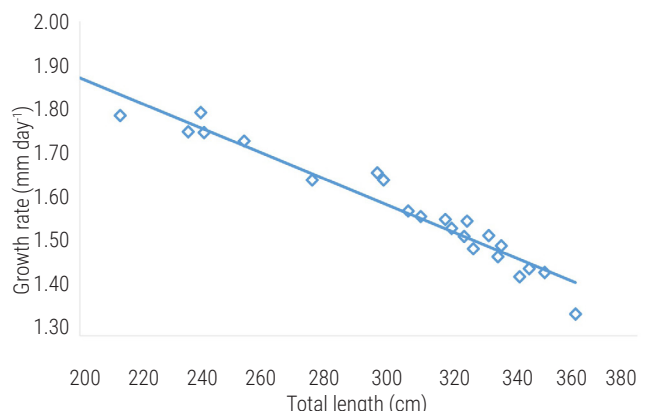
Fig. 4. Transverse section of sagittal otolith with nucleus (*T. auriga*)

from 107 to 267 days. The total length (TL) at age data were best described by an exponential growth function (Table 2). The relationship between TL and age was expressed as: $TL = 37.307 + 0.0054^{eAge}$ ($R^2 = 0.99$) (Fig. 5), while the relationship between body weight (BW) and age was expressed as: $BW = 94.957 + 0.0344^{eAge}$ ($R^2 = 0.829$) (Fig. 6). Daily growth in body weight ranged from 0.05 g BW day⁻¹ to 0.16 g BW day⁻¹. Daily growth rate (DGR) in length varied between 1.34 mm day⁻¹ and 1.85 mm day⁻¹ (Fig. 7). Future studies incorporating larger sample sizes to cover a wider range of sizes and ages will improve the interpretation of pearly hairtail growth, enabling the conversion of annuli counts into distinct age classes (Francis et al., 1992). To date, no comparable studies have been reported on the longevity and early growth of *T. auriga*, limiting direct comparisons with the present findings. However, several age and growth studies are available for the closely related species *T. lepturus*. Hamada (1971) determined the age and growth of *T. lepturus* using transverse sections of otoliths; while Al-Nahdi et al. (2009) reported a maximum age of approximately 7 years based on counting growth rings on the sagittal otolith, with a maximum observed total length of 126 cm. In the East China Sea, *T. lepturus* exhibited an age composition of 2 to 4 years, with maximum recorded ages of 4 years for males and 6 years for females (Kim et al., 2011). Similarly, individuals collected from the southern East China Sea, were reported to range from 0-4 years of age, with TL ranging between 692 to 1826 mm (Shih et al., 2011). Clain et al. (2023) reported a maximum age of 8 years for *T. lepturus* from south-eastern Australia with specimens attaining a TL of up to 193 cm.

Biological characteristics of *T. auriga*

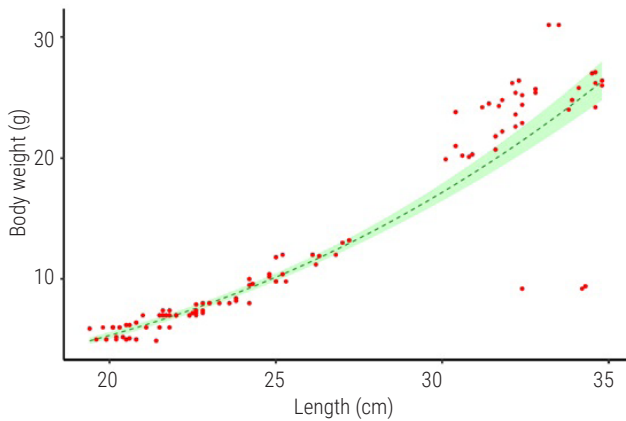
Length-weight relationship (LWR)

In the study, a total of 800 samples in the size range 190-370 mm TL were analysed for determining the LWR. LWR parameters of *T. auriga* was estimated for the pooled stock, yielding 'a' and 'b' values of 0.000955 and 2.88 respectively. Linearising the two variables (length and weight) by taking their logarithmic values and then regressing them gave the linear expressions of LWR for the pooled stock as; $\ln W = \log (-6.954) + 2.88 \log L$ ($R^2 = 0.89$) (Fig. 8). The

Fig. 5. Relationship between TL and age of *T. auriga* from the Arabian SeaFig. 6. Relationship between body weight and age of *T. auriga* from the Arabian SeaFig. 7. Relationship between TL and daily growth rate (DGR) of *T. auriga* from the Arabian SeaTable 2. Models of growth curves fitted to *T. auriga* from the Arabian Sea

Function	TL/No. of increments			BW/No. of increments		
	a	b	R ²	a	b	R ²
Linear	0.9308	-86.921	0.97	5.964	74.659	0.820
Power	0.0417	1.4775	0.98	44.404	0.4953	0.800
Exponential	37.307	0.0054	0.99	94.957	0.0344	0.829

regression coefficient 'b' is less than 3 indicating a negative allometric growth for pooled sexes and was statistically proved by testing with a null hypothesis $H_0: b = 3$ against the alternate hypothesis $H_1: b \neq 3$. The results indicated that the estimated b value (2.88) did not differ significantly from the cubic value of 3 ($p > 0.05$). Since the p value exceeded the set significance threshold, the null hypothesis ($b = 3$) could not be rejected, confirming that *T. auriga* exhibits an isometric length-weight relationship.

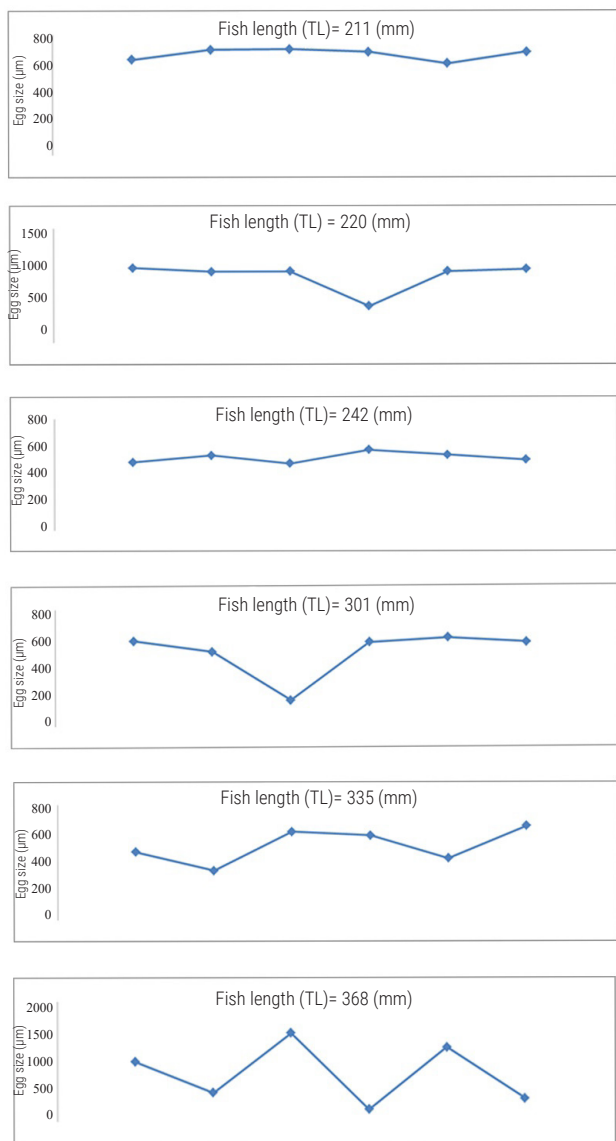
Fig. 8. LWR of pooled samples of *T. auriga*

LWR derived for *T. auriga* in the present study represents the first detailed estimate for this species. However, similar studies on other ribbonfish species such as *T. lepturus* (Reuben *et al.*, 1997), and *Lepturacanthus savala* (Chakravarthy *et al.*, 2012) from the Arabian Sea indicate that, the LWR generally aligns with isometry or a slight negative allometry ($b \leq 3.0$), where deviations are influenced by species-specific and environmental factors.

Fecundity and maturity

A total of 12 fishes ($n = 12$) were selected for fecundity analysis, with TL ranging from 210 to 368 mm and total weight (TW) from 20.8 g to 28.4 g. The fecundity of *T. auriga* was estimated to range from 320–710 eggs per fish. Egg diameter varied between 633 and 1,233 μm , and gonadal histology confirmed maturity stages corresponding to mature, ripe/spawning and spent phases. Importantly, all specimens examined were found to be in mature condition. Although specimens smaller than 190 mm TL were unavailable during the sampling period, this limitation itself provides critical biological insight. Across a three-year sampling window (2022–2024) of ribbonfish landings in this region, no immature *T. auriga* smaller than 190 mm TL were encountered. The smallest individuals collected (190 mm TL) were already histologically mature, with well-developed vitellogenic oocytes, indicating that first maturity is attained at or below 190 mm TL. Therefore, based on our dataset and cumulative field evidence, the size at first maturity of *T. auriga* is inferred to be less than 190 mm TL, demonstrating very early maturation. This aligns with Silas and Rajagopalan (1974), who reported spent and recovering ovaries at 241 mm TL (92 mm snout vent length) and noted that the actual maturity length may be even smaller. Compared with related trichiurids such as *T. lepturus* (47–48 cm TL) (Prabhu, 1955) and *L. savala* (~40 cm TL) (Gupta, 1967), *T. auriga* shows a uniquely low size at first maturity, highlighting a life-history strategy adapted for rapid recruitment within deep-sea slope habitats. Owing to the limited availability of specimens below 190 mm TL, the present study could not precisely estimate the length at first maturity. This limitation highlights the need of a thorough re-estimation of the length at first maturity for *T. auriga*, particularly in comparison with earlier estimates ($L_{m50} = 260$ mm) by Abdussamad *et al.*, (2023). The relationship between egg diameter and TL is shown in Fig. 9.

The histological assessment of maturity stages in female and male specimens based on the available samples is presented below.

Fig. 9. Ova diameter distribution in *T. auriga* showing the prevalence of large sized oocytes in individuals with TL ranging from 211 to 368 mm

Females

Spawning capable (Stage V- Mature, Stage VI - Ripe/ Spawning)

Fish with spawning capable ovaries ($n=15$) ranged from 203 to 368 mm TL, 20.8 to 28.4 g in total weight (TW) and gonad weight (GW) ranged from 0.5 to 2.4 g. Ovaries extended the entire length of the ventral cavity and were characterised by an elongated, spindle-shaped, and yellowish appearance with conspicuous blood vessels. The ova are spherical, fully packed and opaque due to the granular yolk deposition, and visible to the naked eye. Biopsy samples, revealed most of the ova were in the size range of 450–650 μm and were present in good numbers. Histological examination revealed well developed vitellogenic oocytes, characterised by increased

yolk granules deposition with in the cytoplasm and a progressive increase in oocyte size. Histological sections revealed presence of primary oocytes (PG), with most of the gonad at the tertiary vitellogenic (Vtg 3) stage, exhibiting germinal vesicle breakdown (GVBN), and post-ovulatory follicles (POFs). The fully ripe ovary along with representative photomicrographs of oocytes and the corresponding histological stage is shown in Fig. 10 (a,b,c).

Spent or regressing ovary

Fish with regressing ovaries (n=20), of size 19.9 to 34.8 cm in TL, and 5.0 to 26.4 g in TW and 0.1 to 0.4 g GW were examined. The ovaries were transparent, orange-yellowish with barely visible blood vessels and a bloodshot appearance. During this phase, oocytes are large and translucent with a diameter of 600-750 μ m. Primary growth oocytes (PG), cortical alveolar ova (CA), and post-ovulatory follicles (POFs) were visible in histological sections. Tissues predominantly comprises post-ovulatory follicles (POFs) and hydrated oocytes (H). Hydrated oocytes were large and found to be uniform as a result of cytoplasm being filled with fused, hydrated yolk mass. The spent or regressing ovary along with representative micrographs of oocytes and the respective histological stage, is shown in Fig. 10 (d,e,f).

Males

Spawning capable

Fish (n=7) with testes in spawning capable phase ranged from 24.3 to 32.4 cm TL and 9.6 to 23.8 g in BW and the GW ranged from 0.5 and 1.4 g. At this stage, testes usually extend the full length of the ventral cavity and were pale pink to cream in colour with tapered edges. Active spermatogenesis was evident, with the tissue predominantly composed of spermatozoa (Sz) within the

spermatogenic cysts. Histological observation also revealed the presence of secondary spermatocytes (Sc2) and spermatids (St) (Fig. 11. a,b,c).

Spent/Regressing

Fish with regressing testes (n=11) ranged from 19.8 to 34.3 cm in TL and 4.9 to 12.0 g in BW and GW ranged between 0.1 g and 0.4 g. Testes appeared cream coloured, small and flaccid. Histological examination revealed a reduced volume of residual spermatozoa (Sz) within the sperm duct-sinus system (SDSS), along with the presence of a few primary spermatogonia (Sg1) located at the periphery of stained sections of the regressing testes (Fig. 11. d,e,f).

The maturity assessed using histological studies allowed for precise identification of gonadal maturation stages of *T. auriga* as it captured subtle cellular changes which are critical for determining reproductive status (West, 1990; Brown-Peterson et al., 2011). The presence of hydrated oocytes and post-ovulatory follicles confirmed that, fish is a batch spawner with asynchronous oocyte development. These findings highlight the protracted spawning season and the reproductive strategy of the species, which is well suited to maintaining population resilience in variable environmental conditions (Murua and Saborido-Rey, 2003).

This study provides the first detailed biological and fishery-level assessment of the pearly hairtail *T. auriga* from the southern coast of India, thereby establishing a critical baseline foundation for its sustainable utilisation. The relevance of this resource to both fishers and industry is particularly notable. Deep-sea trawlers operating in the south-eastern Arabian Sea increasingly relied on *T. auriga* landings as an auxiliary source of income, especially under conditions of rising fuel costs, fluctuating shrimp and cephalopod catches and prevailing market uncertainties that threaten economic viability.

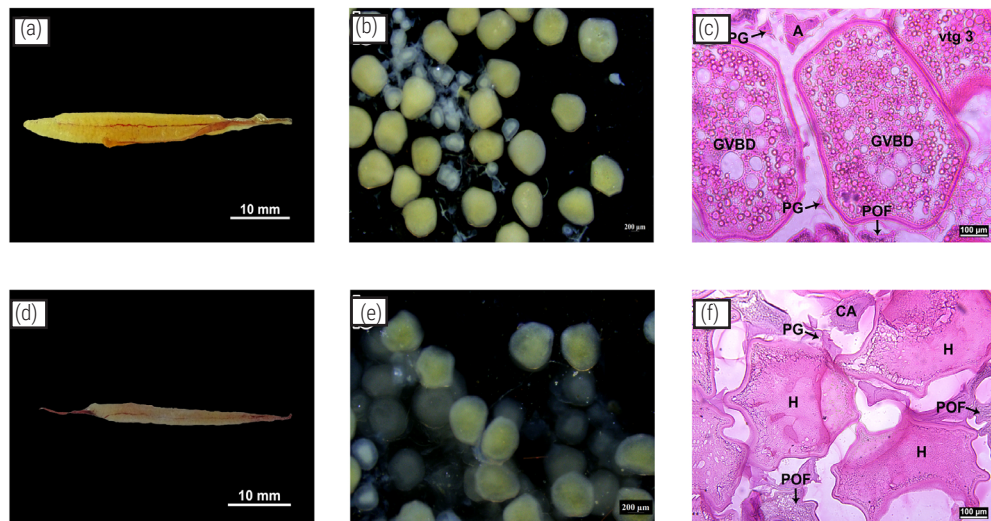


Fig. 10. (a) Spawning capable ovary; (b) Microscopic view of oocytes; (c) Histological section of the spawning capable ovary. (d) Regressing ovary; (e) Microscopic view of oocytes; (f) Histological section of the regressing ovary. PG: Primary growth oocytes; Vtg 3: Tertiary vitellogenic stage; GVBN: Germinal vesicle breakdown; POFs: Post-ovulatory follicles; H: Hydrated oocytes

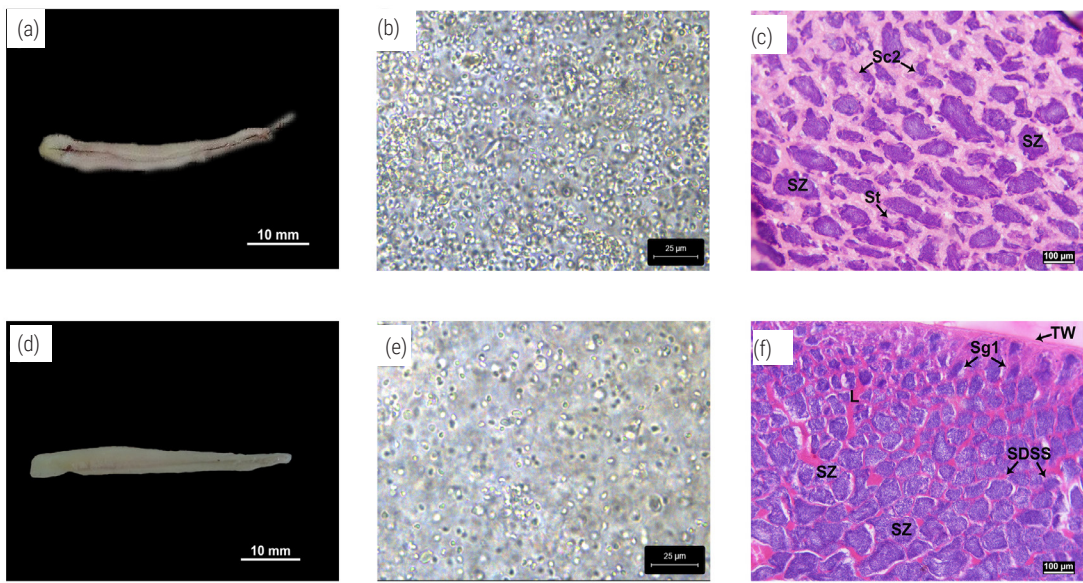


Fig. 11. (a). Spawning capable testes; (b) Microscopic view; (c) Histological section showing the presence of spermatozoa (Sz of testes); secondary spermatocyte (Sc2) and spermatids (St). (d) Regressing testes; (e) Microscopic view of regressing testes; (f) Histological section showing residual spermatozoa (Sz); sperm duct-sinus system (SDSS) and spermatogonia (Sg1)

The fishmeal and fish oil (FMFO) sector has already responded to this resource availability indicating clear market pull and immediate livelihood relevance. For many vessels, *T. auriga* now represents the margin between economic loss and profitability, especially during the final days of multi-day fishing trips when fuel tanks and fish holds are partially empty. Thus, beyond its biological novelty, *T. auriga* represents a high-value functional component of the contemporary fishing economy in southern Kerala and Tamil Nadu.

From an ecological perspective, the findings demonstrate that *T. auriga* possesses a life-history profile distinct from most trichiurid species. Its unusually small size at first maturity suggested by the present study to occur well below 190 mm TL, combined with a continuous or extended spawning window, indicates reproductive adaptation to deep-sea slope environments where episodic recruitment and patchy distribution are common. While such life history traits confer resilience and ensure rapid replenishment of adult biomass, they simultaneously raise management concerns. When the fishable stock is comprised largely of mature individuals, the removal of large seasonal aggregations directly targets the reproductive population, thereby increasing vulnerability to overexploitation during peak fishing windows. Fishers participating in stakeholder consultations reported noticeable seasonal declines in catch volumes within each fishing season (described as "tons per haul early in the season decreasing sharply later"), highlighting a possible depletion pulse within each aggregation cycles. If substantiated, this pattern indicates that the fishery may currently depend on localised seasonal hotspots, which, if repeatedly exploited in the absence of regulatory measures, may undergo depletion similar to the historic small pelagic fishery collapses.

The study also brings attention to a major governance and data challenge arising from the species misidentification. *T. auriga* closely resembles juvenile *T. lepturus* and is often misidentified during landing-site inspections, particularly in context with MLS regulations for *T. lepturus* are enforced. Such misclassification not only distorts catch and effort statistics, but may also result in unwarranted penalties on fishers unintentionally harvesting legally permitted species. This highlights the need for species-specific capacity building measures, including illustrated field identification guides, onboard laminated diagnostic sheets, fisher-training workshops, and if resources permit, the future adoption of low-cost molecular barcoding tools or QR-linked digital identification aids. This preliminary investigation fills a major knowledge gap by quantifying biological traits, estimating growth and reproductive characteristics, and contextualizing fishery behaviour. However, science-based management cannot rely solely on biological snapshots. Future work must expand to:

- Spatio-temporal mapping: Identification of spatial hotspots, seasonal aggregation sites and assessment of whether populations are migratory or regionally resident.
- Fishery-independent surveys: -Estimation of absolute abundance and biomass across slope depths (200–600 m), reducing reliance on landings based data alone.
- Stock structure and genetic delineation: Determination of whether *T. auriga* off Kerala–Kanyakumari coast represents a single stock or multiple localised populations.
- Life-cycle ecology: Tracing early life stages (larvae to juveniles) to determine true maturation habitats and explain the absence of immature individuals in the fishery.

- Socio-economic valuation: Quantification of the income contribution of *T. auriga* to fishing households, FMFO value chains, and coastal employment.
- Adaptive management design: Designing precautionary measures such as seasonal catch thresholds, depth-based access rules, and effort-rotation strategies to guide future expansion of exploitation.

In conclusion, *T. auriga* offers both opportunity and obligation; a new economic frontier for fishers and processors, that simultaneously demands early, science-based stewardship. By integrating strong biological knowledge, continuous fishery monitoring, and active stakeholder participation, India can achieve a forward-looking model of deep-sea fisheries governance, one that balances livelihood security, ecological responsibility, and long-term sustainability of this promising resource.

Acknowledgements

Authors acknowledge Dr A. Gopalakrishnan, Former Director, and Dr. Grinson George, Director, ICAR-CMFRI, Kochi for their guidance and support. Also acknowledge the funding support the India Council of Agricultural Research (ICAR), New Delhi.

References

Abdulsamad, S. M., Jawad, L. A., Al-Nusear, A. N., Waryani, B. and Rutkayová, J. 2020. Asymmetry in the otolith length and width of three sparid fish species collected from Iraqi waters. *Mar. Pollut. Bull.*, 156: 111177. <https://doi.org/10.1016/j.marpolbul.2020.111177>.

Abdussamad, E. M., Abdul Azees, P., Ramachandran, C., Rohit, P., Najmudeen, T. M., Rethesh, T. B., Abbas, A. M., Jesli, D., Sijad, B. and Toji, T. 2023. Pearly hairtail *Trichiurus auriga* Klunzinger: A prospective non-conventional deep-sea resource. *Aquaculture Spectrum*, 6(7): 21–27.

Al-Anbouri, I. S., Ambak, M. A. and Jayabalan, N. 2011. Studies on the age, growth and mortality rates of Indian oil sardine *Sardinella longiceps* Valenciennes, 1847 off Oman Sea, Muscat, Sultanate of Oman. *J. Biol. Agric. Healthc.*, 1(4): 1–8.

Al-Nahdi, A., Al-Marzouqi, A., Al-Rasadi, E. and Groeneveld, J. C. 2009. Size composition, reproductive biology, age and growth of largehead cutlassfish *Trichiurus lepturus* Linnaeus from the Arabian Sea coast of Oman. *Indian J. Fish.*, 56(2): 73–79.

Brothers, E. B. and Mathews, C. P. 1987. Application of otolith microstructural studies to age determination of some commercially valuable fish of the Arabian Gulf. *Kuwait Bull. Mar. Sci.*, 9: 127–157.

Brown-Peterson, N. J., Wyanski, D. M., Saborido-Rey, F., Macewicz, B. J. and Lowerre-Barbieri, S. K. 2011. A standardized terminology for describing reproductive development in fishes. *Mar. Coast. Fish.*, 3(1): 52–70.

Campana, S. E. and Neilson, J. D. 1985. Microstructure of fish otoliths. *Can. J. Fish. Aquat. Sci.*, 42: 1014–1032.

Chakravarty, M. S., Pavani, B. and Ganesh, P. R. C. 2012. Length-weight relationship of ribbon fishes *Trichiurus lepturus* (Linnaeus, 1758) and *Lepturacanthus savala* (Cuvier, 1829) from Visakhapatnam coast. *J. Mar. Biol. Ass. India*, 54(2): 99–101.

Clain, C., Stewart, J., Fowler, A. and Diamond, S. 2023. Reproductive biology of largehead hairtail *Trichiurus lepturus* in south-eastern Australia. *Aquac. Fish.*, 8(2): 148–158. <https://doi.org/10.1016/j.aaf.2021.09.008>

CMFRI 2022. *Status and potential of Indian marine fisheries resources*. ICAR-Central Marine Fisheries Research Institute, Kochi, India

CMFRI 2023. *CMFRI Annual report 2022*. ICAR-Central Marine Fisheries Research Institute, Kochi, India, 252 p.

CMFRI 2024. *CMFRI Annual report 2023*. ICAR-Central Marine Fisheries Research Institute, Kochi, India, 283 p.

Collette, B. B. and Nauen, C. E. 1983. *FAO Species catalogue. Vol. 2. Scombrids of the world. An annotated and illustrated catalogue of tunas, mackerels, bonitos and related species known to date*. FAO Fisheries Synopsis, 125(2). Food and Agriculture Organisation of the United Nations, Rome, Italy, 137 p.

Francis, R. I. C. C., Paul, L. J. and Mulligan, K. P. 1992. Ageing of adult snapper (*Pagrus auratus*) from otolith annual ring counts: Validation by tagging and oxytetracycline injection. *Mar. Freshw. Res.*, 43(5): 1069–1089.

Ganga, U., Beni, N., Jinesh, P. T., Manjebrayakath, H. and Ghosh, S. 2024. Insights from an exploratory survey-based assessment of the deep-sea fish resources of the continental slope in the Indian EEZ. *Mar. Fish. Inf. Serv. T&E Ser.*, 259: 23–34.

Ganga, U., Jinesh, P. T. and Beni, N. 2015. A note on the ribbonfish *Trichiurus auriga*. *Mar. Fish. Inf. Serv. T&E Ser.*, 226: 20–21.

Ganga, U., Muktha, M., Dash, S. S., Rahangdale, S., Wilson, L., Rajesh, K. M., Purushottama, G. B., Mahesh, V., Thomas, S., Ghosh, S. and Kizhakudan, S. J. 2023. Gonad staging for tropical marine finfishes – Good practices and procedures. *Mar. Fish. Inf. Serv. T&E Ser.*, 257: 18–24.

Green, B. S., Mapstone, B. D., Carlos, G. and Begg, G. A. 2009. Introduction to otoliths and fisheries in the tropics. In: Green, B. S., Mapstone, B. D., Carlos, G. and Begg, G. A. (Eds.), *Tropical fish otoliths: Information for assessment, management and ecology*. Springer, Dordrecht, pp. 1–22.

Gupta, M. V. 1967. Studies on the taxonomy, biology and fishery of ribbon fishes (Trichiuridae) of the Hooghly estuarine system, 2. Biology of *Trichiurus savala* Cuvier. *Proc. Zool. Soc.*, 20: 153–170.

Hamada, R. 1971. Age and growth of the ribbonfish *Trichiurus lepturus* Linnaeus based on transverse section of the otolith. *Bull. Seikai Reg. Fish. Lab.*, 41: 53–62.

James, P. S. B. R. 1967. Comments on the four new species of ribbonfishes (family Trichiuridae) recently reported from India. *J. Mar. Biol. Ass. India*, 9(2): 327–338.

Kim, Y. H., Yoo, J. T., Lee, E. H., Oh, T. Y. and Lee, D. W. 2011. Age and growth of largehead hairtail *Trichiurus lepturus* in the East China Sea. *Korean J. Fish. Aquat. Sci.*, 44(6): 695–700.

Le Cren, E. D. 1951. The length-weight relationship and seasonal cycle in gonad weight and condition in the perch (*Perca fluviatilis*). *J. Anim. Ecol.*, 20: 201–219.

Mildenberger, T., Taylor, M. H. and Wolff, A. M. 2017. TropFishR: An R package for fisheries analysis with length-frequency data. *Methods Ecol. Evol.*, 8(11): 1520–1527. <https://doi.org/10.1111/2041-210X.12791>.

Murua, H. and Saborido-Rey, F. 2003. Female reproductive strategies of marine fish species of the North Atlantic. *J. Northwest Atl. Fish. Sci.*, 33: 23–31.

Najmudeen, T. M. 2023. Overview of marine fisheries of India. In: *Course manual, International Workshop-cum-Training on Fisheries management and aquaculture*. ICAR-Central Marine Fisheries Research Institute, Kochi, India, pp. 12–22.

Nakamura, I. and Parin, N. V. 1993. *FAO species catalogue. Vol. 15. Snake mackerels and cutlassfishes of the world*. FAO Fisheries Synopsis, 125(15). Food and Agriculture Organisation of the United Nations, Rome, Italy, 136 p.

Nelson, J. S. 2006. *Fishes of the world*. 4th edn. John Wiley & Sons, Inc., Hoboken, New Jersey, USA, 601 p.

Prabhu, M. S. 1955. Some aspects of the biology of the ribbon fish *Trichiurus haumela* (Forskal). *Indian J. Fish.*, 2(1): 132-163.

Raje, S. G. 1999. Some observations on the biology of *Trichiurus lepturus* (Linnaeus) from Veraval (Gujarat). *Indian J. Fish.*, 46(1): 79-83.

Ramirez-Llodra, E., Tyler, P. A., Baker, M. C., Bergstad, O. A., Clark, M. R., Escobar, E., Levin, L. A., Menot, L., Rowden, A. A., Smith, C. R. and Van Dover, C. L. 2011. Man and the last great wilderness: human impact on the deep sea. *PLoS ONE*, 6(8): e22588. <https://doi.org/10.1371/journal.pone.0022588>.

Reuben, S., Vijayakumaran, K., Achayya, P. and Prabhakar, R. V. D. 1997. Biology and exploitation of *Trichiurus lepturus* Linnaeus from Visakhapatnam waters. *Indian J. Fish.*, 44(2): 101-110.

Ricker, W. E. 1973. Linear regressions in fishery research. *J. Fish. Res. Board Can.*, 30(3): 409-434. <https://doi.org/10.1139/f73-072>.

Sajeevan, M. K. and Nair, J. R. 2006. Distribution and abundance of non-conventional deep-sea finfish resources off the southwest coast of India. *Indian J. Fish.*, 53(3): 345-352.

Shih, N. T., Hsu, K. C. and Ni, I. H. 2011. Age, growth and reproduction of cutlassfishes *Trichiurus* spp. in the southern East China Sea. *J. Appl. Ichthyol.*, 27(6): 1307-1315. <https://doi.org/10.1111/j.1439-0426.2011.01805.x>

Silas, E. G. and Rajagopalan, M. 1974. Studies on demersal fishes of the deep neritic waters and the continental slope. II. On *Trichiurus auriga* Klunzinger, with notes on its biology. *J. Mar. Biol. Ass. India*, 16(1): 253-274.

West, G. 1990. Methods of assessing ovarian development in fishes: A review. *Mar. Freshw. Res.*, 41(2): 199-222.